The Lifecycle of the North Atlantic Storm Track

Lenka Novak, * Maarten HP Ambaum, and Rémi Tailleux

Department of Meteorology, University of Reading, Reading, United Kingdom

* *Corresponding author address:* Lenka Novak, Department of Meteorology, University of Reading, P.O. Box 243, Reading, RG6 6BB, United Kingdom.

E-mail: l.novakova@pgr.reading.ac.uk

ABSTRACT

The North Atlantic eddy-driven jet exhibits latitudinal variability, with evidence of three preferred latitudinal locations: south, middle and north. Here we examine the drivers of this variability and the variability of the associated storm track. We investigate the changes in the storm track characteristics for the three jet locations, and propose a mechanism by which enhanced storm track activity, as measured by upstream heat flux, is responsible for downstream latitudinal shifts in the jet. This mechanism is based on a nonlinear relationship between baroclinicity and meridional high-frequency (periods of shorter than 10 days) eddy heat flux, which induces an oscillatory behaviour of these two quantities. Such oscillations in baroclinicity and heat flux induce variability in eddy anisotropy which is associated with the dominant type of wave breaking and the northward deflection of the jet. Our results suggest that high heat flux is conducive to a northward deflection of the jet, whereas low heat flux is conducive to a more zonal jet. Since this jet deflection effect was found to operate most prominently downstream of the storm track maximum, the storm track and the jet remain anchored at a fixed latitudinal location at the upstream side of the storm track. These cyclical changes in heat flux and storm track characteristics can be viewed as different stages of the storm track's spatio-temporal lifecycle.

1. Introduction

A key feature of terrestrial storm tracks is that they are generally accompanied by a deep tropospheric jet primarily driven by the momentum convergence produced by the storm tracks' high-frequency baroclinic eddies (Hoskins et al. 1983). This three dimensional momentum convergence can be visualised using the divergence of the **E**-vectors (Hoskins et al. 1983). The **E**-vector indicates the direction of eddy propagation and is defined as

$$\mathbf{E} = \left(\overline{v'^2 - u'^2}, -\overline{u'v'}, \frac{f}{\theta_p}\overline{v'\theta'} \propto \overline{v'T'} \right), \tag{1}$$

where the first two terms are the horizontal barotropic components, and the last term is the vertical baroclinic component which is proportional to the lower-level meridional heat flux ($\overline{v'T'}$, referred to as hereafter as 'heat flux'). The bar indicates a time average, the prime denotes a perturbation from that average and θ_p refers to the vertical derivative of potential temperature. Hoskins et al. (1983) observe that the **E**-vectors tend to point upwards at the beginning of the storm track and subsequently become more horizontal and meridionally divergent towards the middle of the storm track. This means that at the beginning of the storm track eddies act to reduce the vertical wind shear (and thus baroclinicity), and further downstream the eddies are responsible for horizontal shifts of the jet. The authors also showed that the horizontal **E**-vector components are strongly dependent on eddy anisotropy, such as tilt and aspect ratio. Variability in the eddy anisotropy was further linked to different types of wave breaking by the idealised experiments of Rivière (2009) and Orlanski (2003), corroborating the observations of a northward jet during anticyclonic wave breaking and a southern jet during cyclonic wave breaking (Woollings et al. 2008; Woollings et al. 2010).

The above research suggests that transitions between different dominant types of wave breaking are crucial for altering the downstream course of the jet. Anticyclonic wave breaking is dominant on a sphere by default (e.g., Rivière 2009), which can be seen by studying the structure of the terrestrial eddy-driven jets spiralling towards the poles. Different mechanisms have been suggested for the transitions to the dominance of cyclonic breaking, including increasing the initial cyclonic barotropic shear of the jet (Thorncroft et al. 1993), enhancing the vertical shear in the lower stratosphere (Wittman et al. 2007) and strengthening the lower-level baroclinicity (Orlanski 2003; Rivière 2009). The latter effect is of interest as recent observational and conceptual studies (for example, Thompson and Birner 2012; Ambaum and Novak, in press, referred to hereafter as 'AN') have suggested that the upstream temperature gradient (and thus baroclinicity) is considerably reduced and replenished in time due to the fluctuations in the eddy activity itself. Since baroclinicity provides favourable conditions for eddy growth its reduction, due to the mixing of the temperature gradients by eddies, inhibits further production of the eddy activity, which then allows the baroclinicity to replenish and the cycle repeats (AN). This nonlinear relationship results in an oscillatory behaviour which is concealed in the time-mean picture. We use the above reasoning to hypothesise that this cyclical variability in the eddy activity and baroclinicity should have a dual role in modifying the jet. The first (upstream) role is the erosion of baroclinicity by eddy activity leading to a fluctuating vertical shear. The second (downstream) role is that the cyclical variations in the upstream heat flux cause a different wave breaking type to dominate, inducing latitudinal shifts in the downstream jet.

In order to test these hypotheses linking different properties of the eddy fluxes to the latitudinal variability in the jet, we need some observational characterisation of the latter. Recently, Woollings et al. (2010) and Franzke et al. (2011) demonstrated, based on the analysis of lower-level wind maxima in the ERA-40 reanalysis data, that the latitudinal variations of the jet in the North Atlantic region could be partitioned into three 'persistent' and 'recurrent' regimes, labelled south (S), middle (M) and north (N) regimes. As this partition conveniently characterises the latitudinal variability of the eddy driven jet, it is adopted here to study the spatio-temporal variability of the storm track and flow characteristics.

Section 2 investigates the direct effect of eddy activity variations during the jet regimes on baroclinicity and the associated baroclinic jet structure. Section 3 then explores the downstream effect of the upstream heat flux and baroclinicity variations on the eddy structure, the associated horizontal **E**-vector components and the barotropic deflection of the jet. Section 4 combines these findings and reveals a sequence of different stages of a cyclic evolution, a lifecycle, of the storm track in space and time. We propose that this lifecycle is associated with a latitudinally-fixed upstream pulsation of eddy activity that drives downstream shifts in the latitude of the storm track and the associated jet. A discussion of the transition to lower frequency timescales (as suggested by Benedict et al. 2004) that leads to this lifecycle, as well as the extent to which this mechanism is local, is also provided in section 4, along with concluding remarks.

2. Upstream Baroclinic Effect

The analyses carried out in this and the following sections are all based on the daily-averaged DJF data from the ERA-40 (1957-2002) reanalysis dataset (as per Uppala et al. 2005). The meridional heat flux, calculated using perturbations from a 10-day low-pass running mean, based on Duchon's (1989) Lanczos filter, of vertically averaged (between 700 and 925 hPa) meridional velocity and temperature was used to represent the storm track activity that is associated with high-frequency eddies (Lorenz and Hartmann 2002). To represent baroclinicity the maximum Eady growth rate at 775 hPa (σ), based on vertical zonal wind shear and a variable static stability parameter (as in James 1994), was used:

$$\sigma = 0.31 \frac{f}{N} \frac{\partial u}{\partial Z}, \tag{2}$$

where f is the Coriolis parameter, N is the static stability parameter and Z is the geopotential height. Both heat flux and baroclinicity were partitioned into the three jet regimes using Frame et al.'s (2011) K-means clustering method. This partitioning method is slightly different to that of Woollings et al. (2010) and Franzke et al. (2011), who used partitioning based on the latitudinal variability of the maximum low-frequency zonal wind. The former method was preferred because it does not require the large-scale flow variability to be based on low-frequency filtering, and because it is more robust when applied to different datasets

(Frame et al. 2011).

Fig. 1 shows heat flux and baroclinicity composites for the three jet regimes. Neither the region of maximum heat flux nor the region of enhanced baroclinicity move latitudinally with the jet to any significant extent until the very downstream end of the storm track. This latitudinal confinement is displayed more explicitly in Fig. 2. In terms of intensity, these two quantities are clearly not proportional to each other as may be suggested by the time-mean picture discussed in many studies (e.g., Hoskins and Valdes 1990; Orlanski 1998). Instead, the heat flux intensity increases with the jet's latitude, whereas the baroclinicity is greatest for the M regime and lowest for the N regime, as is evident from Fig. 2.

Franzke et al. (2011) propose that the preferred transitions between the jet regimes are from M to N, N to S and S to M regimes. Assuming this sequence of transitions, the above temporal relationship between heat flux and baroclinicity is reminiscent of that proposed by AN that was described in the introduction. In their study a large but short-lived (lasting approximately 2 days) heat flux event erodes baroclinicity, which eventually limits further baroclinic instability and the associated heat flux. The reduced heat flux then allows diabatic forcings to replenish baroclinicity until heat flux starts to increase again and the cycle repeats. We suggest that this nonlinear oscillator model can also assist in the interpretation of the variability of heat flux and baroclinicity on the longer (approximately weekly) timescale of the jet regimes. The issue of timescales will be further addressed in the next section. An additional difference is that while AN used the unfiltered $v'T'$ to study short-lived spike-like heat flux events, here we are using its time-filtered value, $\overline{v'T'}$. The latter is proportional to the vertical **E**-vector component and can therefore be easily related to the existing theoretical frameworks. The time-filtered heat flux can be viewed as an accumulation of smaller heat flux events (or a particularly large one). We therefore propose a mechanism by which explosive cyclonic growth is initiated during the M regime due to its high baroclinicity. The cyclones then develop further during the N regime whilst reducing baroclinicity to very low values, followed by a recovery of baroclinicity during the S regime when the eddy activity is limited

(Rivière and Orlanski 2007). This mechanism and its influence on deflecting the jet will be further examined in the next section.

3. Downstream Barotropic Effect

Since Rivière's (2009) study suggests that variations in baroclinicity can lead to different types of wave breaking, the above nonlinear oscillatory relationship between baroclinicity and heat flux should be reflected in different dominant types of wave breaking during the jet regimes. In particular, the N regime is expected to exhibit more enhanced anticyclonic breaking whereas the S regime is expected to be dominated by cyclonic breaking. The different types of breaking would then modulate the horizontal **E**-vector components and thus their influence on the speed and direction of the jet. This section will investigate the extent to which such modulation is observed.

Orlanski's (2003) study proposes that anticyclonic breaking is dominant if the cyclonic eddies are more southwest-northeast (SW-NE) tilted and meridionally elongated, while cyclonic breaking is more characteristic of rounder cyclonic eddies tilted in the southeast-northwest (SE-NW) direction. Different types of wave breaking were thus identified here using Ertel PV on the 315 K isentrope, eddy tilt (α) and aspect ratio (ϵ) along the rotated coordinates relative to the eddy tilt. The two latter quantities were calculated for the 250 hPa level as per James (1994):

$$\alpha = \frac{1}{2}\tan^{-1}\left(\frac{2\overline{u'v'}}{\overline{v'^2} - \overline{u'^2}}\right), \tag{3}$$

$$\epsilon = \frac{\overline{(u'\sin\alpha + v'\cos\alpha)^2}}{\overline{(u'\cos\alpha - v'\sin\alpha)^2}}, \tag{4}$$

where the eddy tilt represents the angle between the minor axis of a meridionally elongated eddy and the circle of latitude, with positive values representing a SW-NE eddy tilt.

As shown in Fig. 3, eddies exhibit a SW-NE tilt on the equatorward side and a SE-NW tilt on the poleward side of the jet in all regimes, as they supply momentum towards the jet core. However, it is clear that the tilting of the N regime is least meridionally confined and seems to have a larger area of positive tilt in the eastern half of the North Atlantic sector. The tilting patterns of the S and M regimes are more meridionally constrained across the basin with the SE-NW tilting on the poleward side of the jet being more extensive during the S regime. The aspect ratio maximum does not change much in magnitude between the regimes but it seems to move more upstream and northwards with increasing jet latitude. The maximum of the N regime is particularly extensive, reaching well into the region of SE-NW tilting. This would imply that enhanced stretching of eddies also occurs on the poleward side of the jet during this regime, whereas it appears to be rather limited on the poleward side of the jet during the other two regimes.

Using Orlanski's (2003) theory, these patterns of eddy shape and tilt indicate that the N regime experiences anticyclonic breaking further upstream and more extensively than the other two regimes. The S regime has the most extensive cyclonic component with the two types of tilting being symmetric along the jet axis. The M regime appears to be strongly influenced by both types of wave breaking.

In support of these interpretations, Fig. 4 shows a composite for the upper-level Ertel PV distribution for the three regimes. It is apparent that the basin-wide ridge tilts in the SE-NW direction for the S regime and in the SW-NE direction for the N regime, suggesting cyclonic and anticyclonic breaking respectively. While such PV patterns may suggest that the most northerly deviation in the flow occurs during the S regime, studying the 2 PVU line (which represents the dynamical tropopause) clearly shows that the upper level jet follows a more pronounced trough-ridge structure and lingers around 60°N during the N regime, whereas it seems to be further south and more zonal for the other two regimes. This figure also shows that PV patterns do not vary to any significant extent outside of the North Atlantic region, indicating statistical robustness of our results as well as the fact that the far upstream flow is not systematically linked to these regimes. Similar and more pronounced patterns have been observed in absolute vorticity distribution (not shown), which additionally indicates both types of breaking during the M regime.

By the **E**-vector definition (Eq. 1), variability in eddy tilt and aspect ratio reflects variability in the horizontal **E**-vector components (Hoskins et al. 1983; Orlanski 1998). These components, however, do not vary in the same manner. For example, the zonal component can be altered considerably by meridional stretching and zonal thinning, while the meridional component remains largely unchanged by the form of eddy decay (Orlanski 1998). It was shown by Orlanski (1998) that the meridional **E**-vector component denotes negative meridional momentum flux and its divergence indicates flow acceleration (or deviation if the divergence is not symmetrical about the jet axis), while the zonal component promotes a quadrupole structure in the flow. Combining the averages of these two components organises the flow into a structure reminiscent of the time-mean trough-ridge pattern observed above both the Atlantic and Pacific ocean basins (Orlanski 1998). Not only the divergence of these two components but also their relative magnitude is therefore important for determining the deflection of the jet. Orlanski (1998) additionally found that the zonal **E**-vector component is particularly efficient at deflecting the jet northward in the North Atlantic.

The composites of the **E**-vector components averaged for the jet regimes (Fig. 5) can therefore be used to directly investigate the effect of eddies on the jet's variability in latitude and intensity during these regimes. The large zonal component and the relatively large northward momentum flux of the N regime imply a northward deflection of the jet during this regime, as the trough-ridge structure becomes more pronounced (Orlanski 1998). The meridional momentum flux convergence (not shown) is relatively small for the N regime, indicating a low jet speed. Despite the more intense poleward momentum flux during the M regime, the reduction in the zonal component keeps the jet at a lower latitude than during the N regime. During the S regime both horizontal **E**-vector components are small and approximately symmetrical along the jet axis. Both the M and S regimes have a relatively high momentum convergence (not shown), leading to relatively high jet speeds. These inferences concur with direct observations of upper-level zonal wind from the reanalysis data, implying that the eddies are, at least to some extent, responsible for this variability of the jet latitude and intensity.

The above results suggest that through an upstream effect of reducing the baroclinicity, variability in the heat flux indirectly steers the variability in the jet latitude further downstream. To confirm this directly, the probability distribution function (PDF) of the heat flux was split into the three jet regimes (Fig. 6). It is apparent that the S regime is most dominant when the heat flux is low and the N regime is most dominant when the heat flux is high.

To show that the relationship between the upstream heat flux and the downstream jet deflection also holds inversely, the heat flux PDF was further divided into terciles, which were then used to split the timeseries of the latitudinal profiles of the downstream jet. Averaging the profiles of each heat flux tercile produces three profile composites (Fig. 7). The highest heat flux tercile yields the most northern jet, whereas the lowest tercile yields the most southern jet. The differences between the jet latitudes are not as extreme as those defining the jet regimes (Fig. 2a). This is, however, expected since the latter was partitioned optimally to show the latitudinal deviations of the jet. Additionally, partitioning the PDF into terciles is not wholly representative of the frequency at which the jet regimes occur. In reality, the M regime is found to be most common while the N regime is found to be least common (Franzke et al. 2011). It can nevertheless be concluded that heat flux has a strong downstream barotropic influence on the jet's latitudinal position.

This analysis was repeated using a 5-day cut-off Lanczos filter to define eddies. Although the results were similar, the equivalent figure to Fig. 7 (not shown) showed a less well defined separation between the zonal wind profiles, with the profiles of the high and middle terciles almost merging at the same latitude. This corroborates Rivière and Orlanski's (2007) findings that the intermediate-frequency (with a period between 5 and 12 days) synoptic eddies are strongly associated with anticyclonic breaking and therefore northward deflection of the jet, so that their removal leads to a less well defined northward jet deflection.

A better understanding of the extent to which heat flux affects the downstream behaviour of the flow can be achieved by comparing the flow observed during the jet regimes and that observed for the heat flux terciles. Fig. 8 shows composites of streamfunction anomalies from the climatological mean averaged for the three respective regimes and heat flux terciles. Although somewhat weaker, the heat flux terciles produce meridionally oriented barotropic patterns very similar to those of the jet regimes. The S jet regime therefore corresponds to the lowest tercile, the M regime to the middle tercile and the N regime corresponds to the highest tercile. The upper-level PV and absolute vorticity composites of the heat flux terciles (not shown) also revealed similar behaviour to those of the jet regimes.

It is worth noting that using the unfiltered $v'T'$ (as used in AN) to partition the time-series into heat flux terciles yields streamfunction anomaly composites that produce zonally oriented baroclinic wavetrains (not shown). This implies that the transition from baroclinic to barotropic flow structures is associated with a transition to lower-frequency variability. In other words, while the reduction in the baroclinicity (and thus wind shear) may promptly respond to individual $v'T'$ events, as shown by AN, the barotropic effect significantly shifting the jet's latitude operates predominantly at lower frequencies of the filtered heat flux. In support of this, time composites of the jet latitude centred around the high peaks in $v'T'$ and $\overline{v'T'}$ were plotted in Fig. 9. Only a small change in the jet latitude can be observed for the $v'T'$-centred composite following the short-term dip (of less than 3 days) in baroclinicity, whereas the jet was found to move north by approximately 5° a day after the peak in $\overline{v'T'}$ and a longer term dip (of approximately 6 days) in baroclinicity.

This section suggests that the jet regimes are a result of the longer-term effect of the non-linear equilibration of zonally-oriented synoptic baroclinic eddies. These eddies cumulatively give rise to meridionally oriented patterns (as suggested by Benedict et al. 2004), similar to those in Hannachi et al. (2012) which represent different phases of the North Atlantic Oscillation (NAO) and the East Atlantic Oscillation (EA). This concurs with the results of Athanasiadis and Ambaum (2009), which suggest that the synoptic eddies (associated with propagating wavetrains across the hemisphere) can only contribute to teleconnections through interaction with lower-frequency waves. The jet regime and heat flux tercile sets are not identical, but it can be concluded that high heat flux events are associated with a more northern shift of the jet, whereas low heat flux events are more associated with a southern shift of the jet.

4. Discussion and Conclusions

The results of this study suggest that variations in storm track activity (in particular lower-level meridional heat flux) have a dual effect on the North Atlantic eddy-driven jet, a direct upstream baroclinic effect, weakening the jet's wind shear, and a downstream barotropic effect, resulting in barotropic shifts in the jet's latitude and intensity. The upstream effect is not in a steady state, but oscillates due to a nonlinear relationship between the heat flux and lower-level baroclinicity as proposed by AN, with the preferred transitions between regimes being from M to N, N to S and S to M (as suggested by Franzke et al. 2011). Because the downstream effect is dependent on the upstream effect, both of these variables will oscillate in time. However, these oscillations do not correlate completely due to their inherently different timescales. The upstream erosion of baroclinicity by high heat flux events occurs almost immediately (as shown in AN), resulting in high-frequency correlated variability in both variables. However, this study demonstrated that an accumulation of such events also results in lower-frequency oscillations of both heat flux and baroclinicity, which have an approximately weekly timescale that is similar to that of the jet regimes. While we found that a short-term heat flux event is only followed by a slight shift in the jet latitude, this shift is significantly magnified when an accumulation of such events (or a particularly large one) precedes it.

To examine the mechanism that links the upstream and downstream effects of the baroclinicity erosion by heat flux, we studied the **E**-vectors and investigated eddy anisotropy, absolute vorticity and PV distribution to identify different types of wave breaking during the three regimes. The N regime is most dominated by anticyclonic breaking and the S regime experiences most extensive cyclonic wave breaking, with the M regime exhibiting a strong influence of both wave breaking types, concurring with Franzke et al.'s (2011) study. We further find that this variability in the dominant type of wave breaking (and the resultant momentum fluxes) is consistent with the changes in the lower-level baroclinicity, and appears to be responsible for the changes in the latitudinal location of the jet, following the mechanism proposed by Orlanski (2003). However, a dominant type of wave breaking can persist for longer than an individual eddy, thereby enabling a transition from high- to low-frequency variability (Benedict et al. 2004). This may explain why the jet shifts are much more prominent on the longer (approximately weekly) timescales. The above spatio-temporal changes in eddy properties, propagation and breaking during the jet regimes can be viewed as the lifecycle of the storm track.

As hinted upon in Section 3 and confirmed in previous studies (e.g., Woollings et al. 2010), the jet regimes are related to the teleconnection patterns, such as the NAO and EA. While teleconnections are not the focus of this paper, it is useful to compare our results to the existing literature to strengthen the validity of our conclusions. For example, Pinto et al.'s (2009) analysis of cyclone 'Daria' shows that its onset in the western Atlantic was shortly followed by an increase in the NAO index which, according to Woollings et al. (2010), translates to a northern shift of the jet. Several days later the NAO index decreased as the storm left the upstream region, reflecting the characteristics of the S regime. Similarly, Woollings et al. (2011) find an increase in eddy activity in situ immediately before the onset of enhanced anticyclonic upper-level wave breaking (i.e., northern shift in the jet), without the need of preconditioned flow from the Pacific. In addition, Mailier et al. (2006) emphasize that there is a strong link between teleconnections and clustering of extratropical cyclones, which is associated with changing values of baroclinicity. Further support comes from Feldstein (2003), who suggests that high frequency eddies are essential for driving the NAO. Similarly, Athanasiadis and Ambaum (2010) showed that high-frequency eddies contribute to teleconnection tendencies by a nonlinear transfer from high to low frequencies. All the above studies confirm our conclusion that local variability of eddy activity induces lower-frequency variability in the downstream jet.

Throughout this study we suggest that the cyclic behaviour of the storm track is a purely local phenomenon. However, it is clear (for example, from the timeseries in Fig. 4 of AN) that these storm track lifecycles are irregular and that other sources of variability are present. It is inevitable that the diabatic heating that replenishes the region of enhanced baroclinicity will vary on many timescales. Furthermore, as suggested in the introduction, there are other mechanisms (other than modifying baroclinicity) that can induce transitions between different types of wave breaking and therefore cause latitudinal shifts in the jet. For example, several studies (for instance, Thorncroft et al. 1993; Franzke et al. 2004; Rivière and Orlanski 2007; Pinto et al. 2011) suggest that preconditioning the flow with barotropic shear can play a significant role in determining the polarity of the NAO index (and thus the jet latitude). This study, however, reveals an insignificant variability outside of the North Atlantic basin during the jet regimes, which would imply that the North Atlantic and North Pacific jets are independent on the timescales of the jet regimes (as found, for example, by Blackmon et al. 1984, Ambaum et al. 2001). We speculate that while high-frequency eddies propagate across the hemisphere as zonally-oriented wavetrains (for example, Gerber and Vallis 2007), their enhancement and shaping across the North Atlantic basin is a local phenomenon (Chang et al. 2002) that will affect local patterns of teleconnections and thus induce lower frequency variations in the local jet's latitude. It is nevertheless still possible that the averaging methods employed in this investigation obscured some external variability outside of the North Atlantic. In addition, while Wittman et al. (2004) conclude that stratospheric changes yield a relatively small response of the tropospheric flow, they note that constant exposure during several baroclinic lifecycles may produce a more significant tropospheric response. This aspect was not studied here and requires further attention.

In terms of broader applicability, the anomalous spikes in heat flux can be observed for all terrestrial storm tracks (Messori and Czaja 2013), but not all exhibit the observed trimodal fluctuations in jet latitude (Woollings et al. 2010). For example, the Pacific-North American pattern is largely dominated by the pulsation of the jet rather than the latitudinal shifts, as a consequence of the stationary eddies being dominant (Franzke and Feldstein 2005). It is possible that these fluctuations in jet intensity in the Pacific region are also a result of baroclinicity erosion by heat flux. The two storm tracks do not appear to be significantly correlated, meaning that different timescales would apply. The Southern Hemisphere storm track, on the other hand, would almost entirely depend on transient eddies, with stationary eddies being sparse. More latitudinal shifts would therefore be expected. Additional investigation of these two storm tracks may separate the individual roles played by stationary and transient eddies, and determine more generally their relative contribution to the spatio-temporal lifecycle of the storm track.

Acknowledgments.

Lenka Novak is supported by the U.K. Natural Environment Research Council [grant number NE/K500860/1]. We thank T. Frame for providing the jet regime classification dataset and J. G. Pinto for his comments on an earlier draft of this paper.

REFERENCES

Ambaum, M. H., B. J. Hoskins, and D. B. Stephenson, 2001: Arctic Oscillation or North Atlantic Oscillation? *J. Climate*, **14**, 3495–3507.

Ambaum, M. H. and L. Novak, in press: A nonlinear oscillator describing storm track variability. *Quart. J. Roy. Meteor. Soc.*

Athanasiadis, P. and M. H. Ambaum, 2009: Linear contributions of different time scales to teleconnectivity. *J. Climate*, **22**, 3720–3728.

Athanasiadis, P. and M. H. Ambaum, 2010: Do high-frequency eddies contribute to low-frequency teleconnection tendencies? *J. Atmos. Sci.*, **67**, 419–433.

Benedict, J. J., S. Lee, and S. B. Feldstein, 2004: Synoptic view of the North Atlantic Oscillation. *J. Atmos. Sci.*, **61**, 121–144.

Blackmon, M. L., Y.-H. Lee, and J. M. Wallace, 1984: Horizontal structure of 500 mb height fluctuations with long, intermediate and short time scales. *J. Atmos. Sci.*, **41**, 961–980.

Chang, E., S. Lee, and K. L. Swanson, 2002: Storm track dynamics. *J. Climate*, **15**, 2163–2183.

Duchon, C. E., 1989: Lanczos filtering in one and two dimensions. *J. Appl. Meteor.*, **18**, 1016–1022.

Feldstein, S. B., 2003: The dynamics of nao teleconnection pattern growth and decay. *Quart. J. Roy. Meteor. Soc.*, **129**, 901–924.

Frame, T. H., M. H. Ambaum, S. S. Gray, and J. Methven, 2011: Ensemble prediction of transitions of the North Atlantic eddy-driven jet. *Q.J.R. Meteorol. Soc.*, **137 (658)**, 1288–1297.

Franzke, C. and S. B. Feldstein, 2005: The continuum and dynamics of Northern Hemisphere teleconnection patterns. *J. Atmos. Sci.*, **62**, 3250–3267.

Franzke, C., S. Lee, and S. B. Feldstein, 2004: Is the North Atlantic Oscillation a breaking wave? *J. Atmos. Sci.*, **61**, 145–160.

Franzke, C., T. Woollings, and O. Martius, 2011: Persistent circulation regimes and preferred regime transitions in the North Atlantic. *J. Atmos. Sci.*, **68**, 2809–2825.

Gerber, E. P. and G. K. Vallis, 2007: Eddy–zonal flow interactions and the persistence of the zonal index. *J. Atmos. Sci.*, **64**, 3296–3311.

Hannachi, A., T. Woolings, and K. Fraedrich, 2012: The North Atlantic jet stream: a look at preferred positions, paths and transitions. *Q.J.R. Meteorol. Soc.*, **138**, 862–877.

Hoskins, B., I. James, and G. White, 1983: The shape, propagation and mean-flow interaction of large-scale weather systems. *J. Atmos. Sci.*, **40**, 1595–1612.

Hoskins, B. and P. J. Valdes, 1990: On the existence of storm-tracks. *J. Atmos. Sci.*, **47**, 1854–1864.

James, I. N., 1994: *Introduction to Circulating Atmospheres*. Cambridge University Press, Cambridge, 230 pp.

Lorenz, D. J. and D. L. Hartmann, 2002: Eddy-zonal flow feedback in the Northern Hemisphere winter. *J. Climate*, **16**, 1212–1227.

Mailier, P. J., D. B. Stephenson, C. A. T. Ferro, and K. I. Hodges, 2006: Serial clustering of extratropical cyclones. *Mon. Wea. Rev.*, **134**, 2224–2240.

Messori, G. and A. Czaja, 2013: On the sporadic nature of meridional heat transport by transient eddies. *Quart. J. Roy. Meteor. Soc.*, **139**, 999–1008.

Orlanski, I., 1998: Poleward deflection of storm tracks. *J. Atmos. Sci.*, **55**, 2577–2602.

Orlanski, I., 2003: Bifurcation in eddy life cycles: Implications for storm track variability. *J. Atmos. Sci.*, **60**, 993–1023.

Pinto, J. G., M. Reyers, and U. Ulbrich, 2011: The variable link between PNA and NAO in observations and in multi-century CGCM simulations. *Clim. Dynam.*, **36**, 337–354.

Pinto, J. G., S. Zacharias, A. H. Fink, G. C. Leckebusch, and U. Ulbrich, 2009: Factors contributing to the development of extreme North Atlantic cyclones and their relationship with the NAO. *Clim. Dynam.*, **32**, 711–737.

Rivière, G., 2009: Effect of latitudinal variations in low-level baroclinicity on eddy life cycles and upper-tropospheric wave-breaking processes. *J. Atmos. Sci.*, **66**, 1569–1592.

Rivière, G. and I. Orlanski, 2007: Characteristics of the atlantic storm-track eddy activity and its relation with the north atlantic oscillation. *J. Atmos. Sci.*, **64**, 241–266.

Thompson, D. W. J. and T. Birner, 2012: On the linkages between the tropospheric isentropic slope and eddy fluxes of heat during northern hemisphere winter. *J. Atmos. Sci.*, **69**, 1811–1823.

Thorncroft, C. D., B. J. Hoskins, and M. E. McIntyre, 1993: Two paradigms of baroclinic wave life-cycle behaviour. *Quart. J. Roy. Meteor. Soc.*, **119**, 17–55.

Uppala, S. M., P. W. Kallberg, A. J. Simmons, U. Andrae, V. D. Bechtold, M. Florino, and et al., 2005: The era-40 re-analysis. *Quart. J. Roy. Meteor. Soc.*, **131 (612)**, 2961–3012.

Wittman, M., A. Charlton, and L. Polvani, 2007: The effect of lower stratospheric shear on barclinic instbility. *J. Atmos. Sci.*, **64**, 479–496.

Wittman, M., R. Scott, and A. Charlton, 2004: Stratospheric influence on baroclinic lifecycles: Connection to the Arctic Oscillation. *Geophys. Res. Lett.*, **31 (16)**, doi: 10.1029/2004GL020503.

Woollings, T., A. Hannachi, and B. Hoskins, 2010: Variability of the North Atlantic eddy-driven jet stream. *Quart. J. Roy. Meteor. Soc.*, **136**, 856–868.

Woollings, T., B. Hoskins, M. Blackburn, and P. Berrisford, 2008: A new rossby wave–breaking interpretation of the North Atlantic Oscillation. *J. Atmos. Sci.*, **65**, 609–626.

Woollings, T., J. G. Pinto, and J. A. Santos, 2011: Dynamical evolution of North Atlantic ridges and poleward jet stream displacements. *J. Atmos. Sci.*, **68**, 954–963.

List of Figures

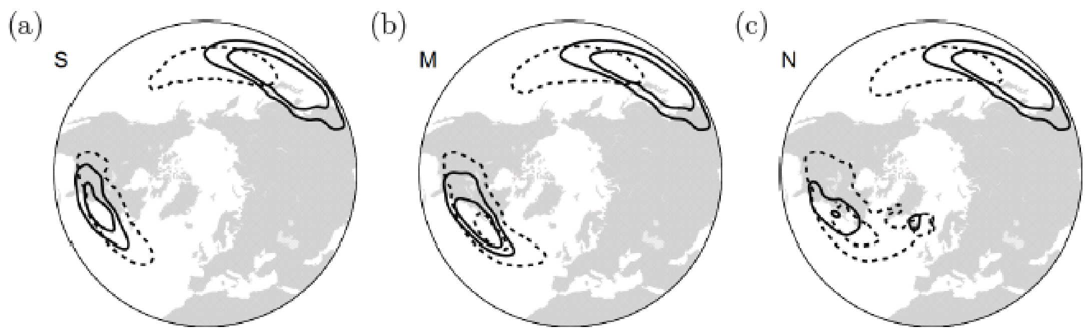

FIG. 1. Hemispheric composites of baroclinicity (solid contours, displaying values of 0.5 and 0.6 days^{-1}) and heat flux (dashed contours, displaying values of 10 and 20 K m s^{-1}) for the S (a), M (b) and N (c) regimes.

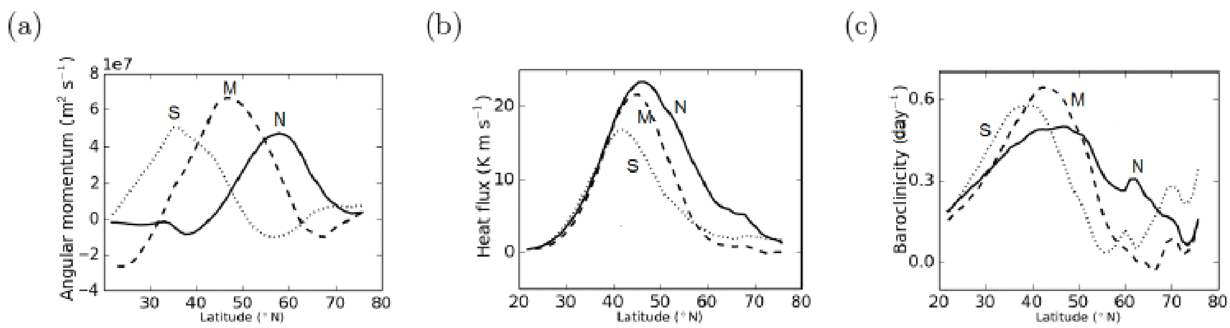

FIG. 2. Composites of latitudinal profiles of relative angular momentum (a, in $m^2\ s^{-1}$ and averaged between 0 and 40°W), heat flux (b, in K m s^{-1} and averaged between 40 and 70°W) and baroclinicity (c, in day^{-1} and averaged between 30 and 90°W) for the S (dotted), M (dashed) and N (solid) regimes.

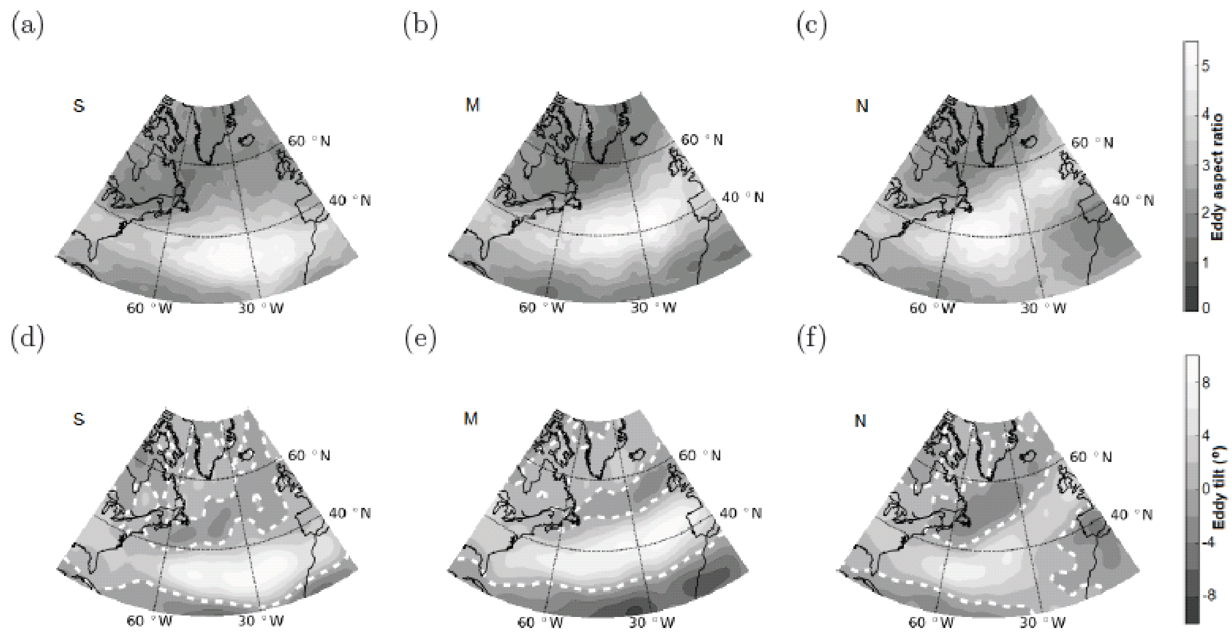

FIG. 3. Composites of the upper-level eddy aspect ratio for the S (a), M (b) and N (c) regimes, and the upper-level eddy tilt for the S (d), M (e) and N (f) regimes. The white dashed line marks the 0° tilt contour.

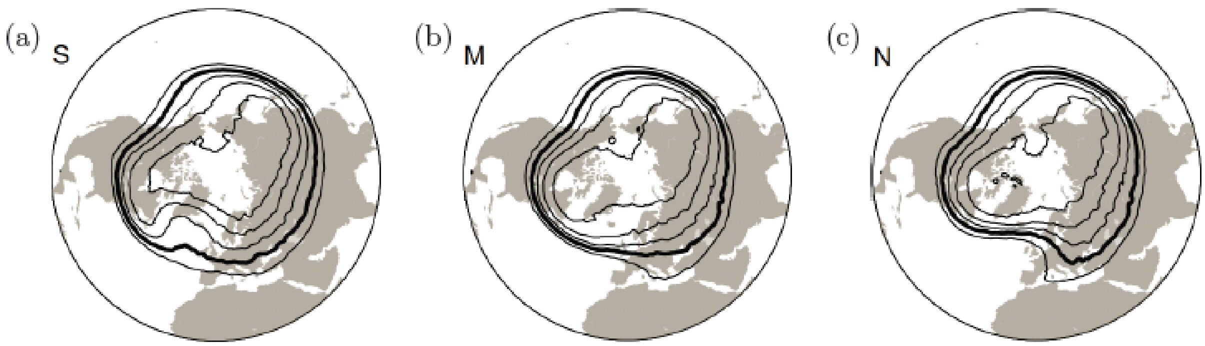

FIG. 4. The median of Ertel PV on the 315 K isentrope for the S (a), M (b) and N (c) regimes. Contours have an interval of 1 PVU and the thick line denotes the 2 PVU contour.

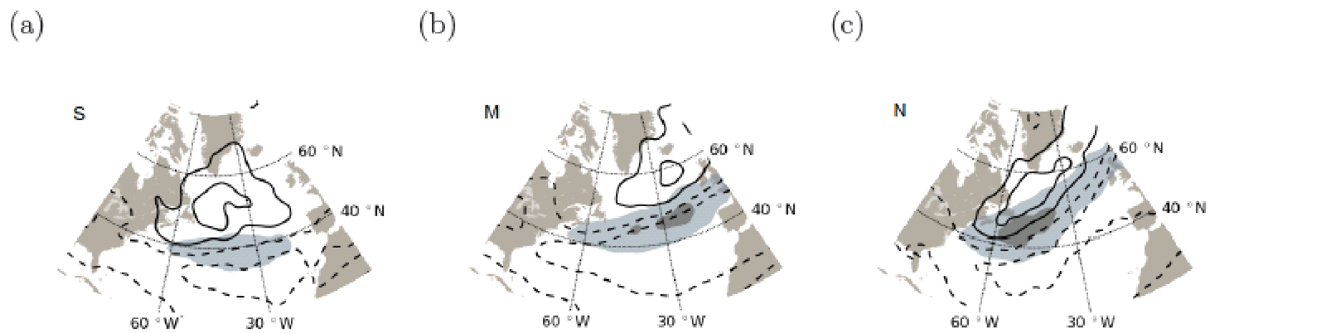

FIG. 5. Composites of the horizontal $\boldsymbol{E}$-vector components for the S (a), M (b) and N (c) regimes. The zonal component is in shaded contours (marking 100 and 150 $m^2\ s^{-2}$), and the meridional component is marked by the solid (10, 25 $m^2\ s^{-2}$) and dashed (-10, -25 $m^2\ s^{-2}$) black contours.

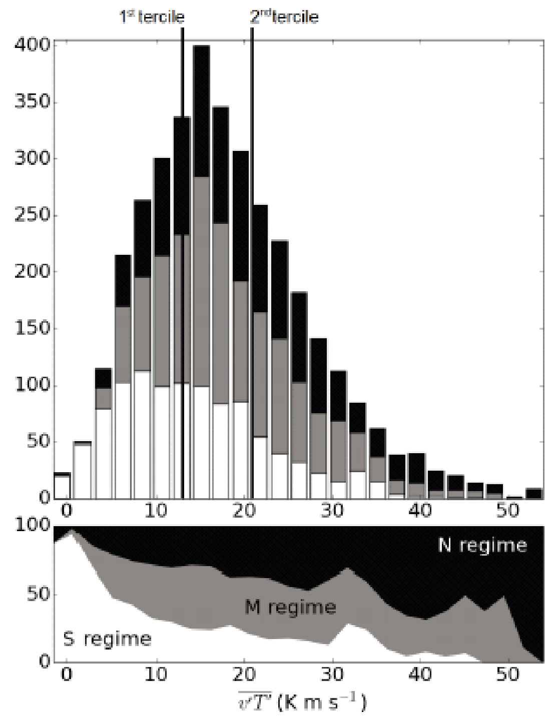

FIG. 6. PDF of the low-pass filtered heat flux (averaged between 40 and 70°W, and 35 and 50°N), showing the occurrences of the S (white), M (gray) and N (black) jet regimes including the division of the PDF into terciles, with the lower panel displaying the relative importance of the regimes (as a percentage) in each bin.

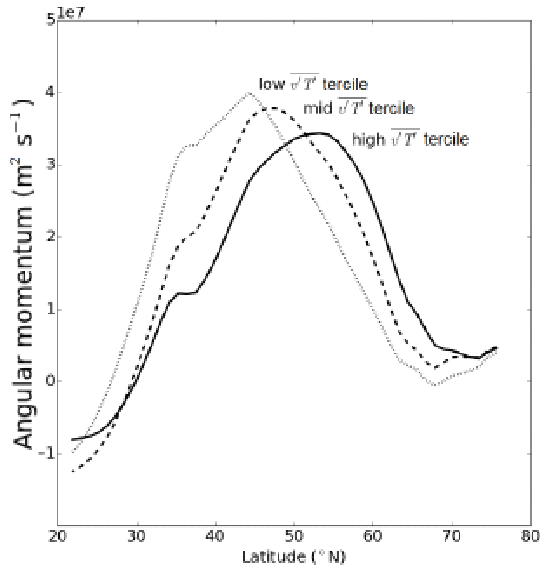

FIG. 7. Composites of the relative angular momentum profiles (averaged between 0 and 30 °W) for the low (dotted line), middle (dashed line) and high (solid line) heat flux terciles.

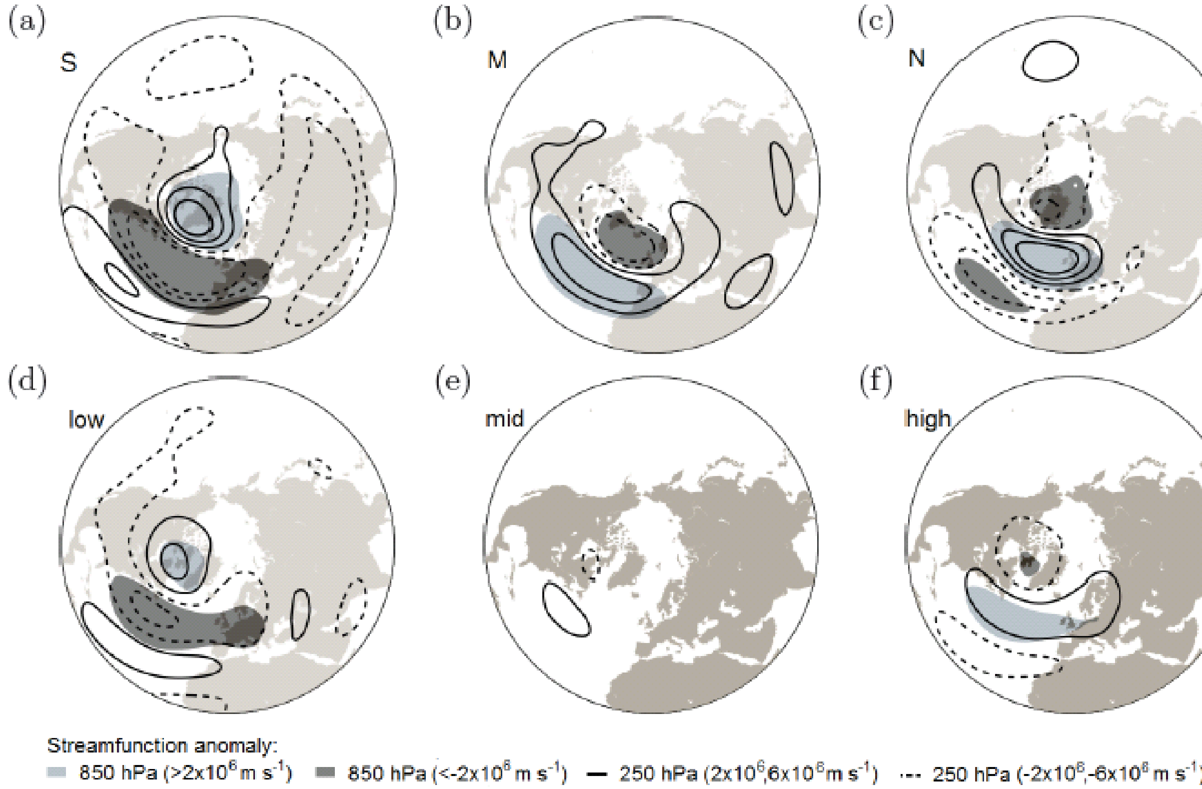

FIG. 8. Composites of the upper-level (250 hPa) and lower-level (850 hPa) streamfunction anomalies for the S (a), M (b) and N (c) regimes and the low (d), middle (e) and high (f) heat flux terciles.

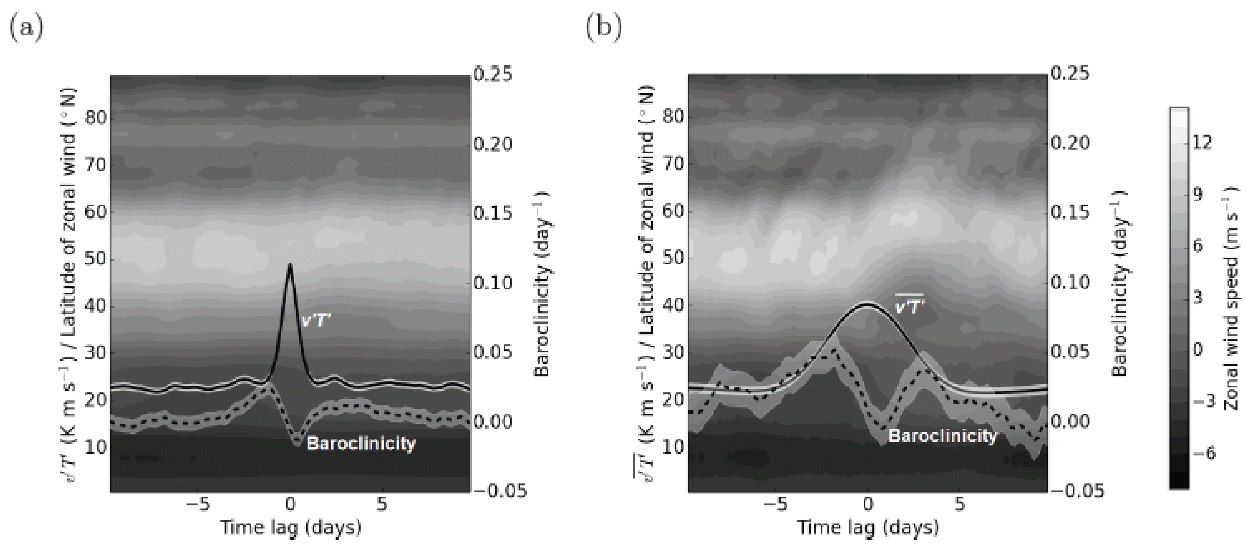

FIG. 9. Composites of the unfiltered (a) and filtered (b) heat flux (solid, averaged between 40 and 70°W, and 35 and 50°N), and baroclinicity (dashed, averaged between 30 and 90°W, and 30 and 50°N). The composites are centred around the maxima (higher than 30 K m s^{-1}) of the respective heat flux variables. Baroclinicity is offset by 0.50 day^{-1} and light shading indicates the standard mean errors. Composites of the zonal wind (averaged between 30 and 0 °W) are marked by the grey-scale filled contours.